

X-ray photoemission characterization of $\text{La}_{0.67}(\text{Ca}_x\text{Sr}_{1-x})_{0.33}\text{MnO}_3$ films

P. R. Broussard, V.M. Browning, and V. C. Cestone
Naval Research Lab, Washington, DC 20375

The Curie temperature and x-ray photoemission spectra of thin films of $\text{La}_{0.67}(\text{Ca}_x\text{Sr}_{1-x})_{0.33}\text{MnO}_3$ (LCSMO) have been studied as a function of the Ca/Sr ratio. The films were grown by off-axis cosputtering from individual targets of $\text{La}_{0.67}\text{Ca}_{0.33}\text{MnO}_3$ (LCMO) and $\text{La}_{0.67}\text{Sr}_{0.33}\text{MnO}_3$ (LSMO) onto (100) oriented NdGaO_3 substrates. The films grow with a (100) orientation, with no other orientations observed by x-ray diffraction. For the alloy mixtures, the Curie temperature, T_C , varies slowly as the Ca/Sr is decreased, remaining ≈ 300 K, while for the LCMO and LSMO films T_C is 260 and 330 K, respectively. The Mn-O valence structure is composed of two dominant peaks, whose positions undergo a change as the Ca fraction is decreased. The core lines behave as linear combinations of lines from pure LCMO and LSMO.

I. INTRODUCTION

The effect of dopants on the photoemission from the lanthanum based manganese oxides has been an area of intense research activity, but usually the studies have focused on varying the $\text{Mn}^{3+}/\text{Mn}^{4+}$ ratio by changing the trivalent/divalent ion ratio.¹⁻⁴ While a great deal of work on studying magnetic, transport and structural properties of these compounds has looked at fixing the $\text{Mn}^{3+}/\text{Mn}^{4+}$ ratio and varying the size of the dopant atoms, little work has been done on photoemission studies. In this paper we present an *in situ* x-ray photoemission spectroscopy (XPS) study of thin films of $\text{La}_{0.67}(\text{Ca}_x\text{Sr}_{1-x})_{0.33}\text{MnO}_3$ (LCSMO) where the $\text{Mn}^{3+}/\text{Mn}^{4+}$ ratio is fixed while the tolerance factor, which is defined as $t = (d_{La-O})/\sqrt{2}(d_{Mn-O})$, is varied by the replacement of Ca with Sr. A similar system was studied by Hwang et al.,⁵ where the variation in the peak and Curie temperature for bulk samples of the CMR materials $\text{A}_{0.7}\text{A}'_{0.3}\text{MnO}_3$ (where A is a trivalent rare earth ion and A' is a divalent rare earth ion) were related to changes to the variation in the tolerance factor. In that work, the system $\text{La}_{0.7}(\text{Ca}_x\text{Sr}_{1-x})_{0.3}\text{MnO}_3$ was studied, and exhibited a change in t from ≈ 0.915 to 0.93 and Curie temperature from 250 to 365 K as x went from 1 to 0.

II. SAMPLE PREPARATION AND CHARACTERIZATION

The samples were grown by off-axis cosputtering onto (100) oriented neodymium gallate (NdGaO_3) substrates using composite targets of LCMO and LSMO material under similar conditions as our previous work.⁶ The LCMO target was radio frequency (rf) sputtered and the LSMO target was direct current (dc) sputtered, giving deposition rates of ≈ 170 -500 $\text{\AA}/\text{hr}$, with film thicknesses being typically 1000 \AA . After deposition, the samples were cooled in 100 Torr of oxygen, and when the samples had cooled to below 100 C, they were moved into a XPS analytical chamber. The chamber pressure during XPS measurements was below 2×10^{-9} Torr.

The XPS spectra were taken at room temperature with a Vacuum Generators CLAM 100 analyzer using Mg $K\alpha$ radiation using the same conditions and analysis as in our earlier work.⁶ Photoemission data for all the samples was collected around the Mn 2p doublet, the La 4d and 3d doublet, the O 1s, Sr 3d, Ca 2p, C 1s, Mn 3p lines, and the valence region. In the following figures of XPS spectra, the core level spectra are shown along with their deconvolution into different Gaussian contributions.

In addition to the XPS studies, the samples were characterized by standard $\theta - 2\theta$ x-ray diffraction scans along the growth direction, atomic force microscopy, electrical resistivity measurements (using the van der Pauw method⁸), and magnetization measurements at low fields using a Quantum Design SQUID Magnetometer.

III. RESULTS AND DISCUSSION

In Fig. 1 we show an atomic force microscopy image for a LCSMO film with 61% Ca fraction. For pure LSMO and LCMO films we typically see surface roughness values of ≈ 16 \AA , while for the mixtures the value is typically 28 \AA . Grain sizes are ≈ 500 \AA for the mixtures, while for pure LCMO and LSMO films they are closer to 1000 \AA . Standard x-ray diffraction along the growth direction for LCMO films shows only the presence of peaks from NdGaO_3 , indicating the excellent lattice match of the (100) oriented LCMO to (100) NdGaO_3 . This match is to be expected with the in-plane lattice constants of the pseudo-cubic unit cells of the two materials being 3.87 and 3.86 \AA , respectively. For LSMO films, however, we find that the lattice match is not as good, with an out-of-plane lattice constant constant of 3.89 \AA . This will give a strain in the films with low values of calcium doping. This strain is seen in the increased coercive fields at 10 K for our LSMO films (170 Oe) compared to LCMO films (20 Oe), as seen in Fig. 2.

In Fig. 3 we present the Curie temperatures (T_C) determined from magnetization data for the samples (taken at 400 Oe) as a function of the calcium fraction. We do not see a smooth variation in the Curie temperature, as was seen in the bulk work.⁵ Instead, there seems to be

a clustering of the values around 300 K, with a slight increase as the Sr content is increased, which would increase the tolerance factor. We also observe a decrease in the Curie temperature for $x=0.25$ (where x is the calcium fraction in the sample) which is not expected. We believe this drop is due to disorder in the samples, which is seen in the higher resistivity for this sample (not shown here) and would be consistent with increased strain in the films for lower values of x .

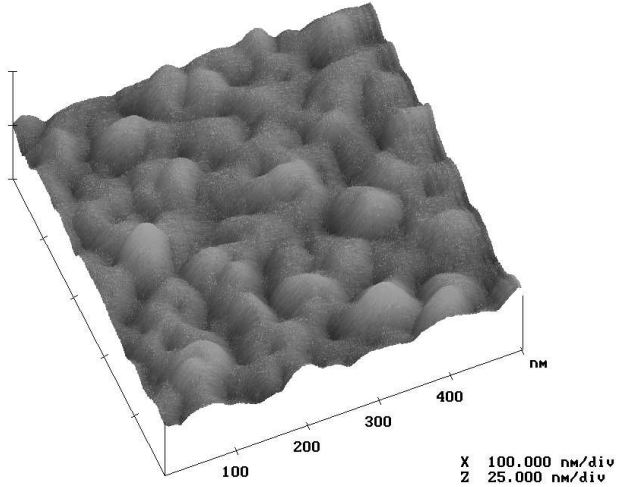


FIG. 1. Atomic force microscopy image for a LCSMO (61% Ca) film grown on (100) NdGaO₃

In Figs. 4 and 5, we show scans around the location of the core lines and low energy region for the LCSMO films for different values of the calcium concentration, x . The curves are offset for clarity. We observe no indication for carbon for these *in-situ* samples, just as in our previous measurements.⁶ For the core lines of Mn, O and La, we see little systematic variation as the Ca/Sr is varied (of the order of 0.1 eV), with the trend being that the peak positions for the core lines of LCMO having a slightly lower energy than LSMO. Peak positions and widths are similar to that seen in earlier XPS studies of LCMO films.^{6,9} The lack of variation in peak position as the Ca/Sr ratio is changed is not surprising, in view of the XPS work on La_{1-x}Sr_xMnO₃,² which showed only slight variations (≈ 0.3 eV in the metallic regime) in the core lines as the Sr fraction changed. Scans of the Ca and Sr core lines show the expected variation in intensity as the Ca/Sr ratio is varied, but again, there is no systematic variation in the peak positions, which for the Sr 3d_{5/2} is 132.0 eV. The peak ratios are similar to that seen in our earlier study on LCMO,⁶ implying that for these systems the terminating layer is MnO₂

In Fig. 5d we show the valence structure for the samples as a function of the calcium fraction. As the calcium fraction decreases, and the samples go from insulating to metallic at room temperature, we observe no change near the Fermi edge, which is similar to that seen in studies on La_{1-x}Sr_xMnO₃.^{2,3} In previous studies of the valence

band of LSMO using XPS,³ a peak at 5.8 eV was observed, which did not change position as the Sr fraction was increased. Instead, a reduction in intensity near 3-4 eV was observed, which was interpreted as being due to changes in doping. For our system, we are not changing the filling of the $e_{g\uparrow}$ band, since we are keeping the doping fixed. However we are changing the overlap integral as the value of t is varied. We also find we can fit the valence structure to a doublet structure, as shown in Fig. 5. As the samples go from pure Sr to pure Ca doping, we find the low and high energy peaks change from 2.7 to 2.9 eV, and 5.6 to 6.0 eV, respectively. This trend in peak positions is opposite that seen for the core lines, which tend to lower their energy in going from LSMO to LCMO. We do not observe any systematic changes in spectral weight in the valence region as the samples go from pure LSMO to LCMO.

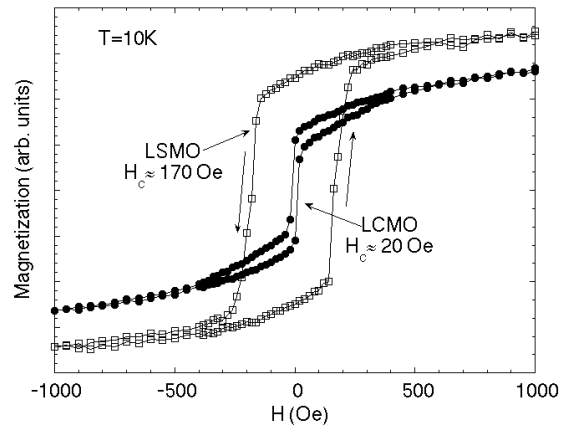


FIG. 2. Hysteresis loop at 10 K for pure LCMO and LSMO films

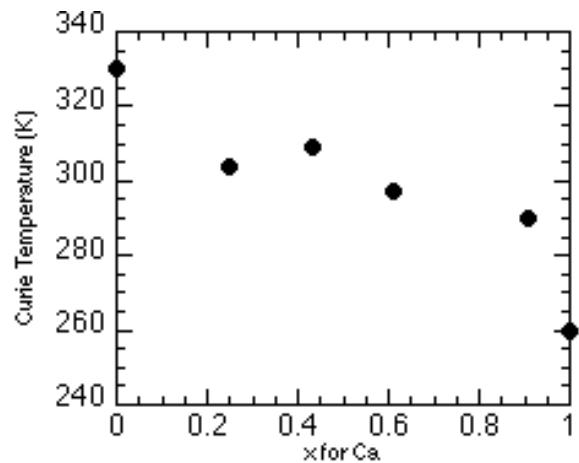


FIG. 3. Curie temperature vs. calcium fraction for LCSMO films grown on (100) NdGaO₃.

IV. CONCLUSIONS

Thin film alloy mixtures of (100) oriented $\text{La}_{0.67}(\text{Ca}_x\text{Sr}_{1-x})_{0.33}\text{MnO}_3$ have been grown and have somewhat rougher surfaces and smaller grain sizes than seen for pure LSMO or LCMO. The Curie temperature for the films does not follow the expected smooth variation as the calcium fraction is changed, which we interpret as being due to disorder. We believe this disorder is caused by strain in the films which is observed in both X-ray diffraction and coercive field measurements. The core lines in XPS measurements behave as linear combinations of individual LCMO and LSMO films, with no significant change in position as the Ca/Sr ratio is varied. The intensity ratios of the peaks is similar to previous work indicating that the terminating layer for the films is MnO_2 . The low energy valence structure exhibits a doublet character, whose peak positions decrease as the Ca fraction is reduced. We interpret this change as being due to variations in the overlap integral between the Mn 3d and O 2p orbitals.

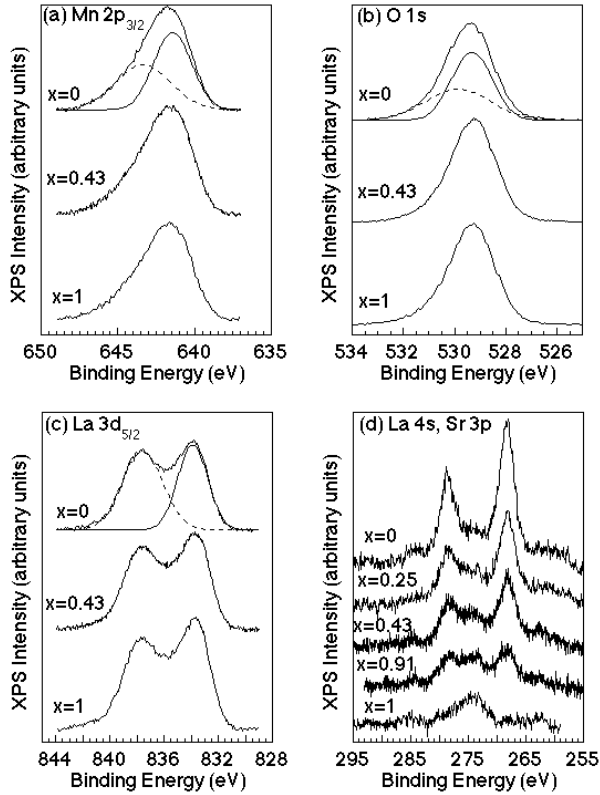


FIG. 4. XPS spectra and peak fit analysis of (a) Mn $2p_{3/2}$, (b) O 1s, (c) La $3d_{5/2}$, and (d) La 4s, Sr 3p and C 1s lines. Spectra are shown for various values of the calcium concentration, x .

V. ACKNOWLEDGMENTS

We would like to gratefully acknowledge the assistance of Michael Miller for the AFM measurements and Andrew Patton in the production of the films.

- ¹ T. Saitoh, A. Sekiyama, K. Kobayashi, T. Mizokawa, A. Fujimori, D.D. Sarma, Y. Takeda, and M. Takano, Phys. Rev. B **56**, 8836 (1997).
- ² T. Saitoh, A. E. Bocquet, T. Mizokawa, H. Namateme, M. Abbate, Y. Takeda, and M. Takano, Phys. Rev. B **51**, 13942 (1995).
- ³ A. Chainani, M. Matthew and D.D. Sarma, Phys. Rev. **B47**, 15397 (1993).
- ⁴ H. Taguchi and M. Shimada, J. Sol. St. Chem. **67**, 37 (1987).
- ⁵ H.Y. Hwang, S-W. Cheong, P.G. Radaelli, M. Marezio, and B. Batlogg, Phys. Rev. Lett. **75**, 914 (1995).
- ⁶ P.R. Broussard, S.Q. Qadri, V.M. Browning and V.C. Costone, Appl. Surf. Sci **115**, 80 (1997).
- ⁷ D. A. Shirley, Phys. Rev. **B5**, 4709 (1972).
- ⁸ L. J. van der Pauw, Phillips Res. Rep. **13**, 1 (1958).
- ⁹ R.P. Vasquez, Phys. Rev. B **54**, 14938 (1996).

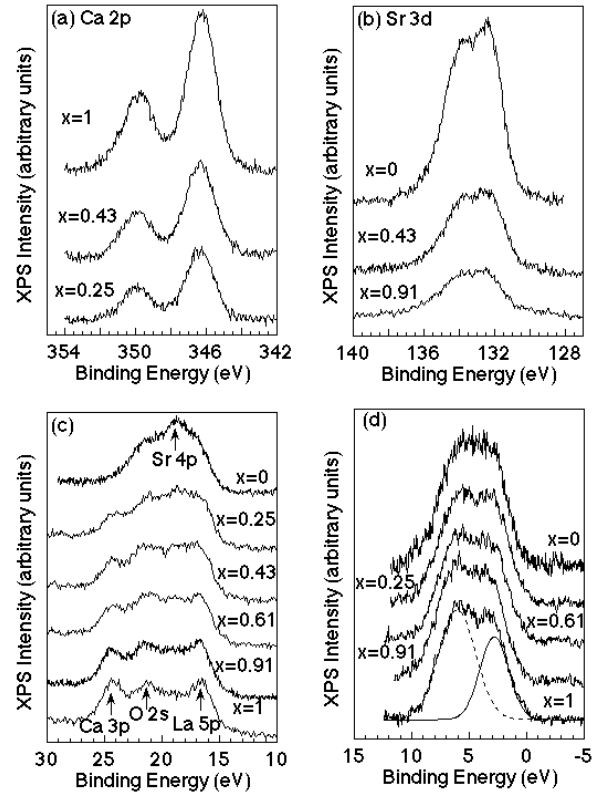


FIG. 5. Same as Figure 4 but for (a) Ca 2p, (b) Sr 3d, (c) the low energy core lines, and (d) the valence region.